663. OFS '93

Optical Fibre Sensor for High Pressure Measurement Using an in-Fibre Grating

M. G. Xu, L. Reekie, Y. T. Chow and J. P. Dakin

Optoelectronics Research Centre, Unversity of Southampton
Southampton SO9 5NH, United Kingdom

Abstract

A fibre optic sensor for monitoring high pressures, using an in-fibre grating, has been constructed. The method involves tracking the wavelength of peak reflection from an in-fibre grating as it is pressurised. Experimental trials, under the influence of hydraulic pressure, have been carried out and a wavelength shift of 0.22 nm at 70 MPa pressure was observed. The sensor should be an attractive choice for ultra-high pressure monitoring.

1. Introduction

Fibre optic Bragg grating sensors have been reported for the measurement of both temperature and strain[1]. A very important aspect of sensors based on gratings is their simplicity, small size and the relative ease and convenience of monitoring a number of sensing elements formed in a single length of fibre[2]. They are interrogated in the spectral domain, and therefore sensing systems based on them are relatively immune to changes in transmission of the fibre network. In this paper, we report the first optical in-fibre-grating pressure sensor and we shall present results for the pressure and temperature response. We will then compare the pressure and temperature sensitivity of the sensor with that theoretically expected and also with that recently achieved with our novel hollow-microsphere pressure sensor[3].

2. Sensor Construction

An illustration of the construction of our high pressure sensor is shown in Fig.1. Light from a 1550 nm fibre-pigtailed ELED is coupled, via a directional fibre coupler, into the sensor head, which is simply a monomode fibre with an in-fibre grating. This photo-refractive grating was written holographically with U.V. light and had a peak reflectivity of 0.8, and a bandwidth of 0.7 nm at a wavelength of 1533.3 nm. The sensing probe was installed within a cavity in a high pressure vessel. Hydraulic pressure was applied to compress the fibre and change the spatial period and reflectivity of the grating. The reflectance of the probe was monitored using a commercial optical spectrum analyser (ANDO AQ-6310B), located to receive light from a return port of the coupler. Undesirable reflection from the unused output port of the coupler was suppressed using index-matching oil, whereas that from the end of the fibre with the grating was suppressed by immersion in the hydraulic oil itself. The hydraulic pressure system consisted of a hydraulic pump, a commercial precision pressure transmitter (Druck PDCR 960) and a purpose-designed pressure vessel, capable of being used up to 70 MPa.

3. Pressure Sensing Theory and Results

When the fibre is compressed the Bragg wavelength varies, mainly due to a combination of (a) a decrease, $\Delta\Lambda$, in the spatial period, Λ, of the grating, and (b) a photoelastically-induced increase, Δn, in the effective refractive index, n, of the fibre core. According to the Bragg condition, the peak reflected wavelength, λ_g, of the grating is proportional to the product of its spatial period, Λ, and its effective refractive index, n. Therefore, the fractional change, $\Delta\lambda_g/\lambda_g$, induced in the Bragg wavelength, λ_g, in response to a pressure change, ΔP, is given by:

$$\frac{\Delta\lambda_g}{\lambda_g}=\frac{\Delta(n\Lambda)}{n\Lambda}=\left[\frac{1}{\Lambda}\frac{\partial\Lambda}{\partial P}+\frac{1}{n}\frac{\partial n}{\partial P}\right]\Delta P \qquad (1)$$

It should be noted that, in the weakly-guided single-mode region, the contribution to the fractional change in optical propagation delay arising from a small fractional change in fibre diameter due to pressure is negligible when compared with the changes in refractive index and physical length. As a result, the fractional change in physical length of the fibre sensor and refractive index of the fibre core, respectively, are given by[4]:

$$\frac{\Delta L}{L} = -\frac{(1-2\mu)P}{E} \tag{2}$$

$$\frac{\Delta n}{n} = \frac{n^2 P}{2E}(1-2\mu)(2p_{12}+p_{11}) \tag{3}$$

where E and μ are Young's modulus and Poisson's ratio of the fibre, respectively, and p_{11} and p_{12} are components of the strain-optic tensor. This of course assumes the fibre is mechanically homogeneous. As the fractional change in the spatial period of the grating equals the fractional change in physical length of the sensing section, the fractional change in the grating spatial period is then given by:

$$\frac{\Delta\Lambda}{\Lambda} = \frac{\Delta L}{L} = \frac{(1-2\mu)P}{E} \tag{4}$$

The fractional change **per unit pressure** in the spatial period and in the refractive index are then given, respectively, by:

$$\frac{1}{\Lambda}\frac{\partial\Lambda}{\partial P} = -\frac{1-2\mu}{E} \tag{5}$$

$$\frac{1}{n}\frac{\partial n}{\partial P} = \frac{n^2}{2E}(1-2\mu)(2p_{12}+p_{11}) \tag{6}$$

The pressure sensitivity, in terms of the fractional change of **Bragg wavelength** per unit pressure, is then given by:

$$\frac{\Delta\lambda_g}{\lambda_g \Delta P} = -\frac{(1-2\mu)}{E} + \frac{n^2}{2E}(1-2\mu)(2p_{12}+P_{11}) \tag{7}$$

Using a value of 7×10^{10} N/m^2 for Young's modulus, Poisson's ratio value of 0.17, values of 0.121 and 0.270 for p_{11} and p_{12}, respectively, for fused silica and a value of 1.465 for the refractive index of the germania-doped core, the predicted fractional wavelength shift becomes:

$$\frac{\Delta\lambda_g}{\lambda_g} = -5.18\times10^{-6}\Delta P \tag{8}$$

where ΔP is the pressure change in MPa. Figure 2 shows the actual spectrum, observed in the wavelength domain, which is reflected from an in-fibre-grating sensing probe. This spectrum shows that the peak reflected Bragg wavelength was 1533.27 nm at zero pressure. From eqn.(5), we would have expected a fractional change in Bragg wavelength of -5.18×10^{-6}/MPa, whereas our measured fractional change was -1.98×10^{-6}/MPa. This was equivalent to a wavelength shift with pressure of -3.04×10^{-3} nm/MPa. As the values of E, μ, p_{11} and p_{12} are likely to be significantly different for the germania-doped silica glass of which the fibre core is composed, we would expect that the most likely reason for the discrepancy is our lack of knowledge of the precise values for Young's modulus, Poisson's ratio and the strain-optic coefficients for the fibre core material.

4. Cross-Sensitivity to Temperature (Theory and Measurement)

The theoretically-expected cross-sensitivity to a change in temperature, ΔT, expressed as a fractional change in wavelength, is given by:

$$\frac{\Delta\lambda_g}{\lambda_g}=\left[\frac{1}{\Lambda}\frac{\partial\Lambda}{\partial T}+\frac{1}{n}\frac{\partial n}{\partial T}\right]\Delta T=(\alpha+\xi)\,\Delta T \qquad (9)$$

where α is the thermal expansion coefficient of the fibre. The effects of fibre diameter change are assumed to be negligible. For our germania-doped fibre core, α is expected to be about $1.1\times10^{-6}/°C$.[5] ξ is the thermooptic coefficient, which has a value of approximately $8.3\times10^{-6}/°C$ for germania-doped silica[6]. We would expect from eqn.(6) that the cross-sensitivity to temperature of the in-fibre grating is $9.4\times10^{-6}/°C$. The measured figure shown in Fig.3 was 0.01045 nm /°C, or $6.72\times10^{-6}/°C$, expressed in terms of the fractional change in Bragg wavelength. Thus our expected cross-sensitivity matches reasonably well with that experimentally observed.

5. Comparison with Our Earlier Hollow-Sphere Sensor

It is interesting to compare the sensitivity of a solid body, such as this fibre-grating sensing element, with that of a hollow type, such as the hollow microsphere type reported earlier[3]. As the mechanical compliance of solid bodies is much lower than that of hollow ones, the fractional change in wavelength with pressure is expected to be much lower for the grating sensor. In fact, the sensitivity of the in-fibre grating with pressure is actually two orders of magnitude lower than we have measured with the hollow microsphere pressure sensor under similar conditions. In the microsphere sensor case, the fractional change in wavelength with pressure was -5.9×10^{-4}/MPa and the temperature coefficient was $4.9\times10^{-6}/°C$. The ratio of the pressure sensitivity to temperature sensitivity for the in-fibre grating sensor was two orders of magnitude worse than for our microsphere type, therefore far more compensation is necessary to correct for temperature changes in the grating type. However, the grating sensor has a distinct advantage for ultra-high pressure measurement, as it should be capable of withstanding enormous hydrostatic pressure, far in excess of that possible with the hollow sphere sensor (The hollow sphere withstood 7MPa), and well above the range covered in these first measurements.

6. Conclusions

We have described a simple fibre optic sensor for monitoring hydrostatic pressure, which uses a monomode fibre, LED source, PIN detector and an in-fibre grating as the sensing element. A Bragg wavelength shift of 3.04×10^{-3} nm /MPa was observed, which is two orders of magnitude lower than we have measured with a hollow microsphere pressure sensor under similar conditions. However, this new sensor is expected to be an attractive, simple and robust-miniature sensor for measuring ultra-high pressure.

7. References

1. W. W. Morey, G. Meltz and W. H. Glenn, "Fibre optic Bragg grating sensors", Proc. SPIE, Vol. **1169**, (1989), p98-107.
2. W. W. Morey, "Distributed fibre grating sensors", Proc. OFS, (1992), p285-288,
3. M. G. Xu and J. P. Dakin, "A novel hollow-glass microsphere sensor for monitoring high hydrostatic pressure", Proc. SPIE, O/E Fiber'92 Boston USA, Conference Track " Fiber Optic and Laser Sensors X ", SPIE Vol, **1795**, paper 2.
4. G. B. Hocker, "Fibre-optic sensing of pressure and temperature", Appl. Opt. Vol.**18**, (1979), p1445.
5. J. Townsend, Private communication.
6. S Takahashii and S. Shibata, "Thermal variation of attenuation for optical fibres", J. Non-crystalline. Solids., Vol **30**, (1979) pp.359-370.

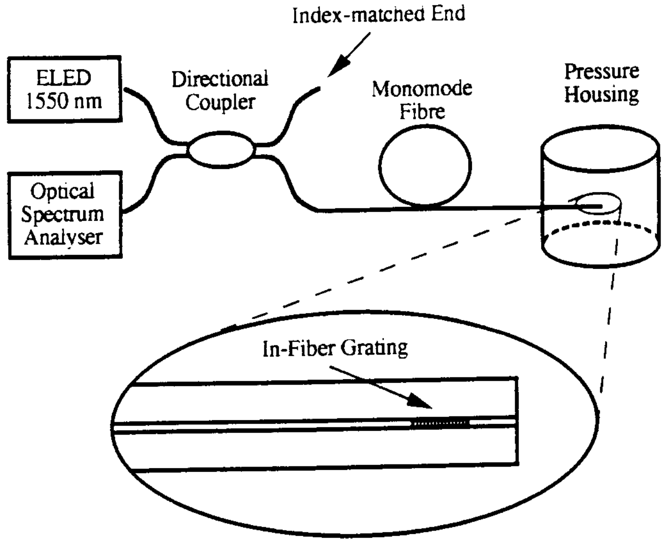

Fig.1 Schematic of In-Fibre Grating Pressure Sensor

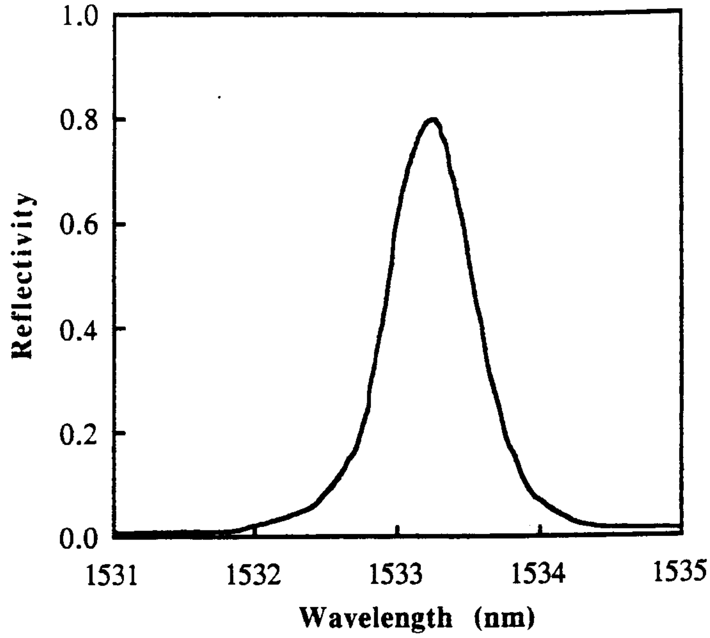

Fig.2 Reflected Spectrum From Sensing Probe

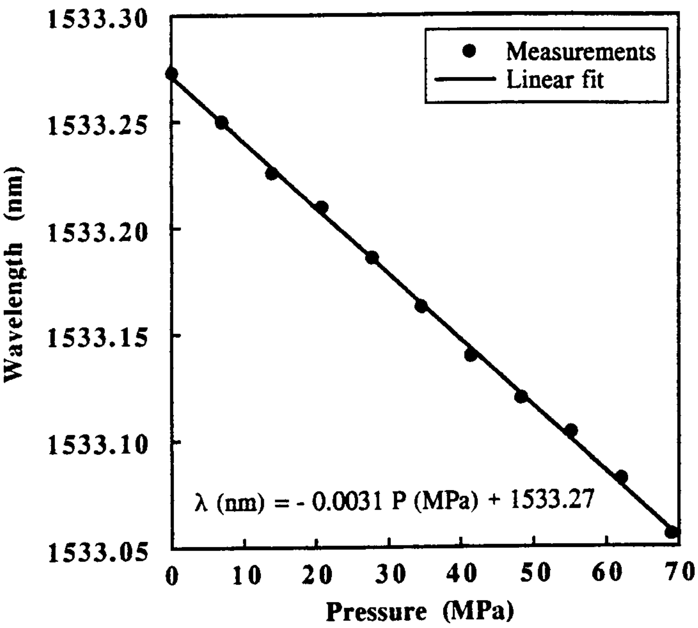

Fig.3 Pressure Response of the Sensor

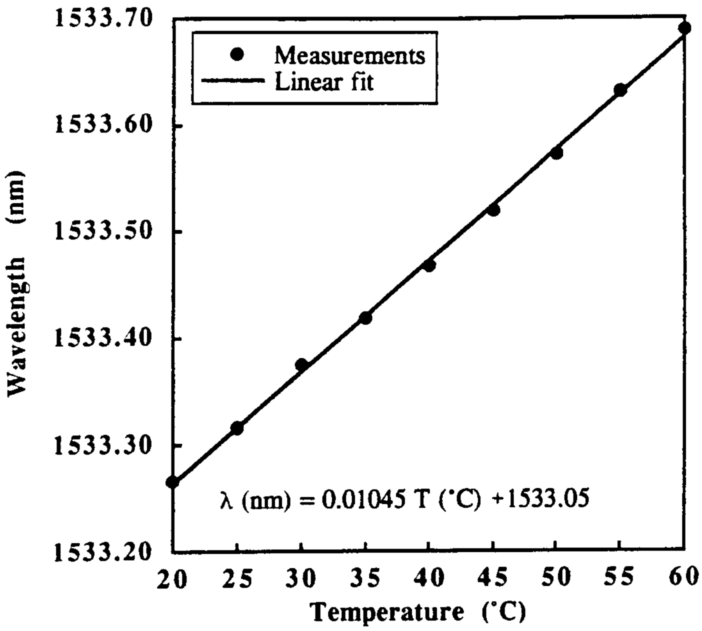

Fig.4 Temperature Response of the Sensor